



Nanohydroxyapatite incorporated photocrosslinked gelatin methacryloyl/poly(ethylene glycol)diacrylate hydrogel for bone tissue engineering

Sreekanth Sreekumaran¹ · Anitha Radhakrishnan¹ · Arun A. Rauf¹ · G Muraleedhara Kurup¹

Received: 17 October 2020 / Accepted: 9 February 2021 / Published online: 26 March 2021
© Islamic Azad University 2021

Abstract

The development of novel strategies that aim to augment the regenerative potential of bone is critical for devising better treatment options for bone defects or injuries. Facilitation of bone repair and regeneration utilizing composite hydrogels that simulates bone matrix is emerging as a viable approach in bone tissue engineering. The present study aimed to develop nanohydroxyapatite-incorporated gelatin methacryloyl (GelMA)/poly(ethylene glycol) diacrylate (PEGDA) hydrogel (GMPH hydrogel). A facile blending and photocrosslinking approach was employed to incorporate nanohydroxyapatite into the inter-crosslinked polymeric hydrogel network to obtain an ECM mimicking matrix for assisting bone tissue regeneration. Chemical characterization of GelMA and the GMPH hydrogel was carried out using FTIR and ¹H NMR. Physical properties of GMPH, such as gelation, swelling and degradation ratios, and internal morphology, signified the suitability of GMPH hydrogel for tissue engineering. Cell viability assay demonstrated a healthy proliferation of MG63 osteoblast cells in GMPH hydrogel extracted growth medium, indicating the hydrogel's cytocompatibility and suitability for bone tissue engineering. Our study documented the fabrication of a novel GelMA/PEGDA-nanohydroxyapatite hydrogel that possesses ideal physicochemical and biological properties for bone tissue engineering.

Keywords Hydrogel · Composite biomaterial · Photocrosslinking · Bone tissue engineering

Introduction

Bone defects and damages arise from multiple risk factors, such as injuries, tumors, and other pathologies, that hamper inherent regenerative mechanisms in bone tissue (Perez et al. 2018). Generally, small defects and wounds in the bone below their critical size heal by bone remodelling (Li et al. 2018). However, medical interventions are required to restore fractured or diseased bone tissue that fails to regenerate by natural means. Autografting and allografting techniques are commonly practiced to treat bone tissue damage. Still, the disadvantages associated with it are inadequate donors, the risks of donor-site morbidity, potential infection, and a higher rate of non-union with host tissues (Li et al. 2018; Liu et al. 2017). There is an urge to develop novel

tissue engineering strategies for assisted bone repair that is fundamentally based on harnessing the innate regenerative potential of native bone. Bone tissue engineering involves a biofunctional paradigm combining polymeric materials with cells, growth factors, and osteoinductive components.

Bone exists as a natural nanocomposite with a mineral phase comprising of hydroxyapatite and an organic phase consisting of Type 1 collagen, non-collagenous proteins, functionally heterogeneous cells, and water (Liu et al. 2016). Different types of bones possess different densities which impart their mechanical properties and function. The outer zone of bone is composed of a dense cortical region, and the inside portion is composed of cancellous bone, which is the spongy part of the bone (Liu et al. 2016). Scientists have been trying to recapitulate bone structure and function using various biomaterials to facilitate tissue regeneration and regain its functionality. These biomaterials have mostly been used across multiple forms, such as scaffolds, hydrogels, nanofibers, etc., as 3D platforms for tissue engineering and regeneration (Hosseinkhani et al.). Lately, bone mimetic scaffolds are designed to facilitate bioactive interactions at

✉ Arun A. Rauf
arunarauf@keralauniversity.ac.in

¹ Department of Biochemistry, University of Kerala,
Thiruvananthapuram, Kerala, India



the tissue biomaterial interface by integrating specific cues for promoting vascularization, osteoinduction, and modulation of host immune defense (Jabbarzadeh et al. 2012; Sabirianpour et al. 2018). Also, scaffolds designed to deliver cells and growth factors at the site of damaged tissue have potential applications in bone tissue engineering (Farokhi et al. 2016).

Hydrogels are physically or chemically crosslinked three-dimensional polymeric structures that absorb and retain large volumes of water without dissolution (Peppas and Hoffman 2020). The tunability of hydrogels makes them suitable templates for delivering growth factors and stem cells for tissue engineering applications (Hernández-González et al. 2020). The 3D architecture of hydrogels enables absorption of water and allows gaseous and nutrient transport mimicking the extracellular matrix (ECM) (Seliktar 2012). Hydrogels with ideal physicochemical properties and biofunctionality promote tissue growth and integration. Despite the wide range of biomedical applications, the hydrogels for load-bearing engineering tissues, such as bone, require unique physicochemical, mechanical, and biological properties. Hydrogels made using synthetic polymers, such as polyglycolic acid, polycaprolactone, polyvinyl alcohol, polyethylene glycol, etc., possess enhanced mechanical properties and are widely employed in tissue engineering applications (Lops et al. 2014). Along with synthetic polymers, proteins, such as collagen (Maisani et al. 2017), gelatin (Nguyen et al. 2016), silk fibroin (Mottaghitlab et al. 2015), and polysaccharides including hyaluronic acid (Hamlet et al. 2017), chitosan (Satpathy et al. 2019), and alginate (Bendtsen et al. 2017), are commonly used in hydrogel constructs to enhance bioactivity and tissue regeneration. Nevertheless, biocomposite scaffolds combining synthetic and natural polymers are considered superior in physicochemical and bioactive properties, such as mechanical stability, biodegradability, biocompatibility, and osteoconductivity (Mohajeri et al. 2010; Stratton et al. 2016; Toosi et al. 2019).

The native extracellular matrix is a collagen-based hydrogel with a complex supramolecular assembly of glycosaminoglycans, proteoglycans, and ECM proteins. Gelatin, which is obtained through the chemical or physical denaturation of collagen, is an excellent choice for fabricating ECM mimics for tissue engineering applications. The presence of Arg–Gly–Asp (RGD) sequences in gelatin facilitates biological interaction between cells and scaffolds (Hoch et al. 2012; Saldin et al. 2017). The gelatin methacryloyl or GelMA has also been considered an ideal candidate in preparing polymeric hydrogels due to its biocompatibility, biodegradability, and chemically tunable properties (Van Den Bulcke et al. 2000; Fang et al. 2016; Hoch et al. 2013; Yue et al. 2017). Though GelMA is known for its ability to enhance osteogenic differentiation of mesenchymal stem cells (Celikkin et al. 2018), the poor mechanical properties

limit its applications in orthopedic tissue engineering. Interestingly, biocomposite hydrogels of GelMA and polyethylene glycol diacrylate (PEGDA) possess mechanical strength and biological properties for bone tissue engineering applications (Wang et al. 2018). Though PEGDA lacks intrinsic biological activity, it is often combined with bioactive polymers to fabricate osteoconductive hydrogel scaffolds. Also, the biocompatible and immunocompatible properties of PEGDA make it an attractive candidate for cell encapsulation, drug delivery, and scaffold-assisted tissue regeneration (Choi et al. 2019).

The incorporation of nanofillers can further augment the mechanical and physical properties of biocomposite materials intended for load-bearing applications (Jamróz et al. 2019). Biosynthetic scaffolds fabricated with nanoscale hydroxyapatite particles as fillers have been reported to induce osteogenic differentiation of stem cells (Lin et al. 2009). Nanohydroxyapatite was shown to enhance fracture tensile stress and compressive strength of the hydrogel. A GelMA/PEGDA hydrogel doped with nanohydroxyapatite has been developed recently as an injectable hydrogel for 3D bioprinting applications. The addition of nanohydroxyapatite provided a mechanically robust composite matrix for bone tissue engineering (Wang et al. 2020). Thus, GelMA/PEGDA hydrogel scaffold reinforced with nanohydroxyapatite can function as a regenerative template for assisted osteoregeneration. The photo-polymerization method is highly desirable for fabricating 3D hydrogel scaffolds and fine-tune their properties to facilitate cell encapsulation and growth factor delivery for enhanced tissue regeneration (Choi et al. 2019). The present study encompasses the fabrication and characterization of a novel nanohydroxyapatite-incorporated photocrosslinked GelMA/PEGDA composite hydrogel for assisted bone regeneration. A facile, blending approach has been adopted for the synthesis of the hydrogels. Cross-linking of polymer constituent was achieved using the photopolymerization technique to obtain stable and reproducible hydrogels with highly tunable properties. The hydrogels' physicochemical and biological properties demonstrated their potential role as ECM mimicking scaffolds for bone tissue regeneration.

Materials and methods

Synthesis of gelatin methacryloyl (GelMA)

GelMA was synthesized as per the previously published protocol (Shirahama et al. 2016). Briefly, a 10% (*w/v*) solution of Type A gelatin (220 bloom; MP Biomedicals) in 0.25 M bicarbonate buffer (pH 9.0) was treated with methacrylic anhydride (Sigma Aldrich) at a feed ratio of 0.1 mL

methacrylic anhydride per gram of gelatin. The reaction was performed at 50 °C for 3 h. The solution was centrifuged, filtered, and dialyzed in ultrapure water for seven days, followed by lyophilization. The dried GelMA foam was stored at –20 °C.

Degree of substitution (DS) of GelMA

Proton NMR (¹H NMR) spectra of GelMA were assessed for calculating the degree of methacrylic group substitution (Hoch et al. 2013). 5 mg of gelatin and GelMA dissolved separately in 650 μL of deuterium oxide (Millipore-Sigma) were analyzed on a Bruker 400 MHz Avance III HD FTNMR spectrometer. The degree of substitution (DS) of the methacrylic group was defined as the percentage of ε-amino groups of gelatin (lysine, hydroxylysine) modified in GelMA. For the quantification of DS by ¹H NMR, the spectra were normalized to the phenylalanine signal (6.9–7.5 ppm), representing gelatin concentration. Subsequently, the lysine methylene signals (2.8–2.95 ppm) of gelatin spectra and GelMA spectra were integrated to obtain the areas [A(lysine methylene of unmodified gelatin)] and [A(lysine methylene of GelMA)]. The DS of the GelMA was calculated as:

$$DS (\%) = \left(1 - \frac{A(\text{lysine methylene of GelMA})}{A(\text{lysine methylene of unmodified gelatin})} \right) \times 100 \quad (1)$$

Fabrication of hydrogels

The photoinitiator, 2-hydroxy-4'-(2-hydroxyethoxy)-2-methylpropiophenone (Irgacure 2959) (TCI Chemicals), was dissolved in PBS at 50 °C. PEGDA (Sigma-Aldrich) was added to this and stirred for 10 min at 50 °C. Finally, GelMA was added and stirred at 50 °C for another 15 min to obtain GMP pre-hydrogel solution (10% w/v GelMA, 10% v/v PEGDA, 0.5% w/v photoinitiator). The solution was sterile-filtered through a polyethersulfone (PES) membrane with 0.22 μm pore size (MDI Membrane Technologies Inc.). UV-sterilized hydroxyapatite (nanopowder < 200 nm particle size, Sigma-Aldrich) was added to GMP pre-hydrogel solution at a concentration of 1% w/v and stirred at 50 °C for 20 min to obtain GMPH pre-hydrogel solution. The pre-hydrogel solutions were layered between glass plates separated with a 1 mm spacer and cross-linked under UV (365 nm) for 5 min to obtain GMP and GMPH hydrogels. The hydrogels are punched out in discs of 1 mm thickness and 8 mm diameter and used for further analysis.

Chemical characterization of hydrogels

The FTIR spectra of gelatin, gel-MA, GMP/GMPH hydrogels between 400 and 4000 cm⁻¹ with a resolution of 0.09 cm⁻¹ were recorded in Thermoscientific Nicolet iS50 spectrophotometer.

Internal morphology of hydrogels

Samples of GMP and GMPH hydrogels were frozen at –80 °C and lyophilized. Cross sections of lyophilized hydrogels were sputter-coated with platinum and scanned using the Carl Zeiss Evo-18 scanning electron microscope. Acquired images were analyzed in ImageJ software to measure the length and width of the pores. The ratio of pore length to width denoted the aspect ratio (Gnanaprakasam et al. 2014).

Gelation and swelling properties of hydrogels

The gelation and swelling properties of the hydrogels were determined according to previously published protocols (Gnanaprakasam et al. 2014; Nurlidar et al. 2018). The hydrogels (1 mm height and 8 mm diameter) were lyophilized and weighed to obtain the initial weight (W_d) and were imbibed in PBS for 48 h at 37 °C to acquire the hydrated weight (W_h). The equilibrium swelling ratio (ESR) and the equilibrium water content (%) (EWC) of the hydrogels were calculated using the following equations:

$$ESR = \frac{W_h - W_d}{W_d} \quad (2)$$

$$EWC (\%) = \left(\frac{W_h - W_d}{W_h} \right) * 100 \quad (3)$$

For gelation ratio (GR), hydrogels were obtained from 100 μL pre-polymer solution. The hydrogels were washed with PBS, and the weight was recorded. The gelation ratio was calculated from the following calculation:

$$GR (\%) = \left(\frac{\text{Weight of the hydrogel}}{\text{Weight of the pre-polymer solution}} \right) * 100 \quad (4)$$

In vitro degradation of hydrogels

The hydrogel samples were freeze-dried, and the dry weight (W_0) was recorded. The hydrogels were immersed in PBS containing collagenase (Type IV, MP Biomedicals) at a concentration of 10 U/mL and incubated at 37 °C. The enzyme solution was replaced every 48 h. On day 7 and day 14, the

hydrogel samples were removed, washed in PBS, freeze-dried, and weighed (W_f). The degradation rate (DR) of the hydrogel scaffolds was obtained from the following calculation:

$$\text{DR (\%)} = \left(\frac{W_0 - W_f}{W_0} \right) * 100 \quad (5)$$

Cell culture

MG63 osteosarcoma cell line was procured from the National Centre for Cell Science, Pune, India. The cells were cultured in a growth medium (DMEM, Gibco) supplemented with 10% heat-inactivated fetal bovine serum (Gibco), $1 \times$ antibiotic–antimycotic solution (Himedia). The cells were maintained at 37 °C in 5% carbon dioxide (CO₂) in a humidified atmosphere in a carbon dioxide incubator. The cells were passaged at 70–80% confluency, and the growth medium was changed every 2 days.

Cell viability assay

The effect of hydrogels on cell viability was studied according to our previously published protocol (Radhakrishnan et al. 2015). The hydrogels were thoroughly washed with sterile distilled water pre-heated at 50 °C to remove traces of unreacted components. Hydrogels were stabilized in a growth medium at 37 °C in a carbon dioxide incubator for 24 h, changing the medium three times. The hydrogel extracts were prepared by incubating the hydrogels in the growth medium (1 disc per mL of medium) at 37 °C in a carbon dioxide incubator (New Brunswick, Eppendorf) for 24 h. Monolayer culture of MG63 cells was initiated at a density of 5×10^3 cells per 24 wells and incubated for 24 h. After incubation, the growth medium was replaced with the hydrogel extracted growth medium and incubated at 37 °C for 24 h. Similarly, the control cells were maintained in the growth medium without hydrogel extract at 37 °C for 24 h. Following incubation, the MTT(3-(4,5-dimethylthiazol-2-yl)-2,5-diphenyltetrazolium bromide; Himedia) assay was performed to calculate the viability of the cells.

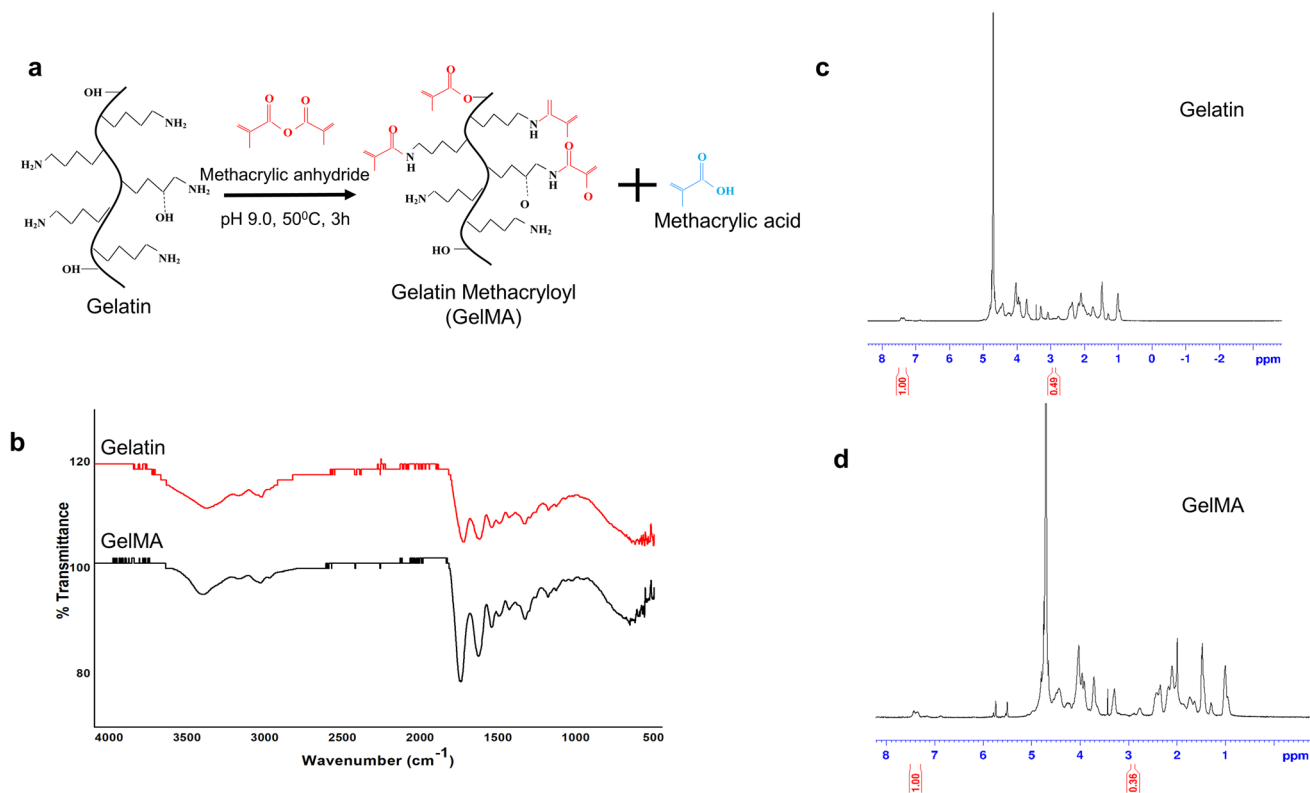


Fig. 1 Synthesis and characterization of GelMA. **a** Gelatin reacts with methacrylic anhydride to give GelMA; **b** FTIR spectra of gelatin and GelMA. **c** ¹H NMR spectra of gelatin. **d** ¹H NMR spectra

of GelMA. The area of the lysine methylene signals (2.8–2.95 ppm) is denoted in the ¹H NMR spectrum



Statistical analysis

Results from six samples from each group were taken for statistical analysis. For pore morphology, a total of 18 pores from each group were analyzed. One-way ANOVA and student *t* test were used to determine statistical significance using GraphPad Prism software. The level of significance (α) was set at $P < 0.05$ for all analyses.

Results and discussion

Hydrogel fabrication

GelMA was synthesized by reacting gelatin with methacrylic anhydride in a precisely controlled set-up described in the methodology. Primary amines of the gelatin are functionalized with methacrylic groups (Fig. 1a). 0.25 M CB buffer in the reaction mix allowed the initial pH of the reaction to be maintained until the reaction was completed. The degree of functionalization of GelMA calculated using proton NMR analysis was 27% (Fig. 1c, d). GMP and GMPH pre-polymer solutions were subjected to UV-crosslinking (365 nm) to obtain GelMA/PEGDA hydrogel with nanohydroxyapatite

dispersed in it. The cross-linking mechanism is illustrated in Fig. 2a. The unsaturated bonds in the methacrylic groups in GelMA and PEGDA undergo photo-polymerization in the presence of photo-initiator resulting in intra- and inter-crosslinked polymeric networks. The incorporation of nano-hydroxyapatite within the GelMA/PEGDA polymeric network further stabilizes the hydrogel.

Fourier transmittance infrared spectroscopy (FTIR)

The FTIR spectrum of GelMA (Fig. 1b) showed a sharp peak at 1230 cm^{-1} representing the C–N stretching of amide groups due to gelatin methacrylation. The band at $1500\text{--}1570\text{ cm}^{-1}$ corresponds to C–N–H bending, while the band at $3200\text{--}3400\text{ cm}^{-1}$ indicates the presence of peptide bonds (mainly N–H stretching) and -OH functional groups. The peak at 1643 cm^{-1} corresponds to C=C stretching in GelMA, suggesting double bonds in the surface (Rahali et al. 2017; Sadeghi and Heidari 2011). The characteristic peaks at 953 cm^{-1} and 1024 cm^{-1} of GMPH correspond to the phosphate groups in hydroxyapatite (Fig. 2b).

Fig. 2 GMPH Hydrogel. **a** Crosslinking mechanism and nanohydroxyapatite incorporation in GMPH hydrogel network; **b** FTIR spectra of GMP and GMPH hydrogel. GMP (GelMA/PEGDA), GMPH (GelMA/PEGDA-nano-hydroxyapatite)

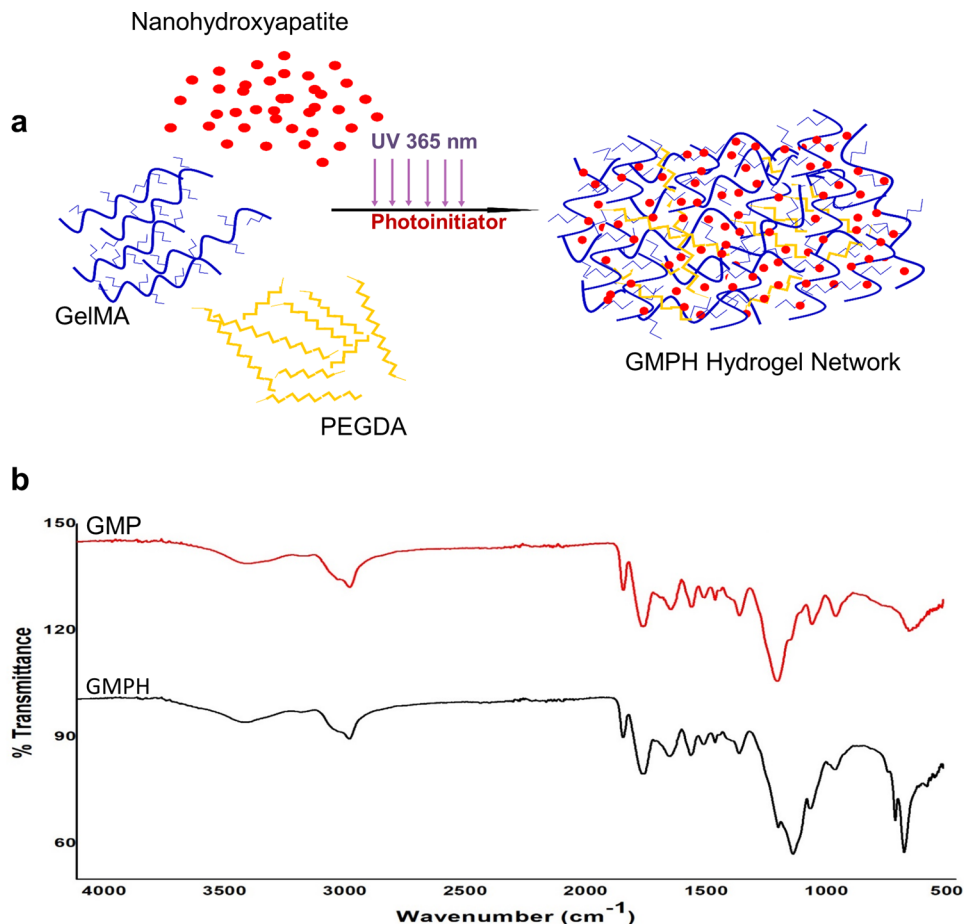
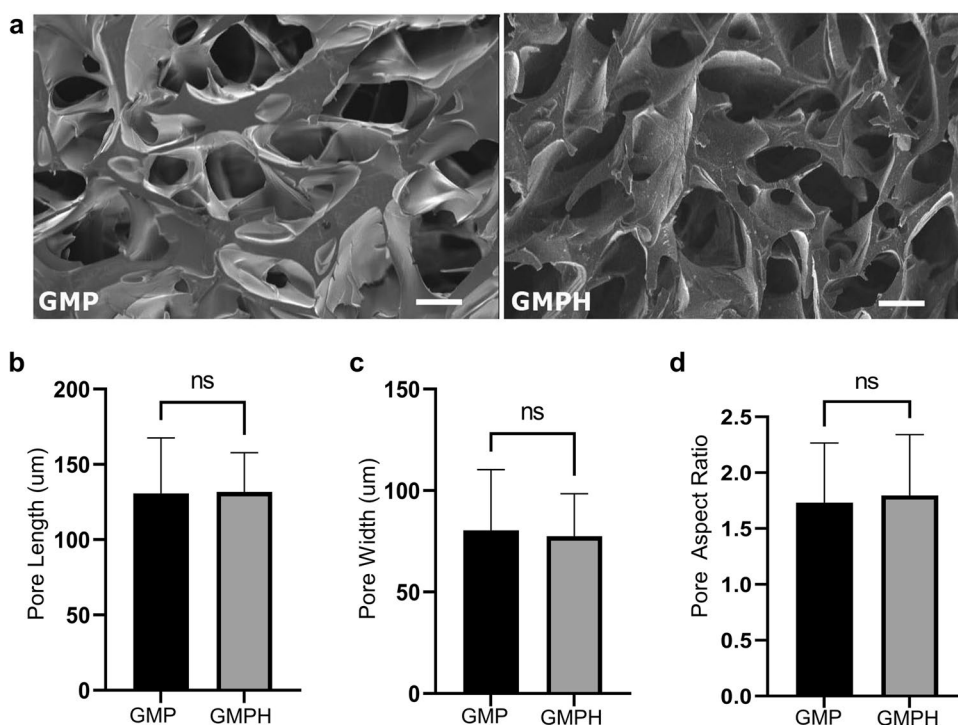


Fig. 3 SEM and pore morphology of GMP and GMPH hydrogels. **a** Internal pore architecture of the hydrogels from SEM images. Calculated average; **b** poreLength ($n = 18$, unpaired two-tailed t test, $P = 0.93$, $*P < 0.05$); **c** pore width ($n = 18$, unpaired two-tailed t test, $P = 0.74$, $*P < 0.05$); **d** pore aspect ratio ($n = 18$, unpaired two-tailed t test, $P = 0.72$, $*P < 0.05$). All error bars represent mean \pm s.e.m. Images were analyzed using ImageJ software. GMP (GelMA/PEGDA), GMPH (GelMA/PEGDA-nanohydroxyapatite)



Pore morphology

Pore size and interconnectivity are vital for the healthy growth of bone tissue. Regeneration of critical bone defects can be hindered by inadequate blood supply, nutrient, oxygen transport, or other pathological conditions (Abbasi et al. 2020). However, scaffolds with porous architecture facilitate cell recruitment and vascularization, allowing the surviving tissue to access sufficient nutrients (Polo-Corrales et al. 2014). The internal porous architecture of the cross sections of hydrogels was obtained from SEM images (Fig. 3a). GMP hydrogels displayed an average pore length of $130.77 \pm 35.76 \mu\text{m}$ and width of $80.41 \pm 30.40 \mu\text{m}$ for GMP hydrogel (Fig. 3b), whereas the GMP possessed an average pore length of $127.7 \pm 95.59 \mu\text{m}$ and width of $67.90 \pm 61.22 \mu\text{m}$ (Fig. 3c). The pore aspect ratios of GMP and GMPH were found to be 1.73 ± 0.53 and 1.79 ± 0.54 , respectively (Fig. 3d). Though a difference in pore length, pore width and pore aspect ratio was observed between GMP and GMPH hydrogels, the results were statistically insignificant. Our findings showed that nanohydroxyapatite particles did not affect the pore morphology of the hydrogel.

Gelation and swelling properties

Physically or chemically crosslinked hydrophilic polymers can function as ideal scaffolds for tissue engineering owing to their ability to swell and form three-dimensional entities for cellular infiltration and growth. The swelling

of hydrogels ensures efficient gaseous and nutrient transport and contributes to mechanical stability (Peppas et al. 2006). GMP and GMPH hydrogels displayed high swelling behavior with ESR ratios of 6.14 ± 0.14 and 5.8 ± 0.27 , respectively (Fig. 4a). The corresponding EWC for GMP and GMPH were 85.99 ± 0.29 and 85.27 ± 0.53 , respectively (Fig. 4b). The results showed that the GMPH hydrogel revealed nearly a 6% drop in EWC and less than 1% drop in ESR than GMP hydrogel. Nanohydroxyapatite has been reported to reduce the swelling properties of hydrogels (Pan 2010). However, the concentration of nanohydroxyapatite (1% w/v) used in this study had a negligible effect on the swelling properties of GMPH hydrogels, as observed by the slight difference in ESR and EWC compared to GMP hydrogel.

The gelation ratio indicates the fractions of GelMA and PEGDA which participate in the cross-linking process (Nurlidar et al. 2018). Our data showed that GMP and GMPH hydrogels possess a gelation ratio of about 77.87% and 75.42%, respectively. This higher percentage of gelation rate indicated a higher fraction of constituent polymers involved in the crosslinking. A 2% fall in the gelation ratio of GMPH can be deemed negligible and implies a lesser interference of nanohydroxyapatite in the gelation process. Though nanohydroxyapatite incorporation resulted in a slight reduction in ESR, EWC, and the gelation rates of the GMPH hydrogel, the differences were not substantial enough to claim that nanohydroxyapatite at 1% concentration disrupts the hydrogel's network structure.

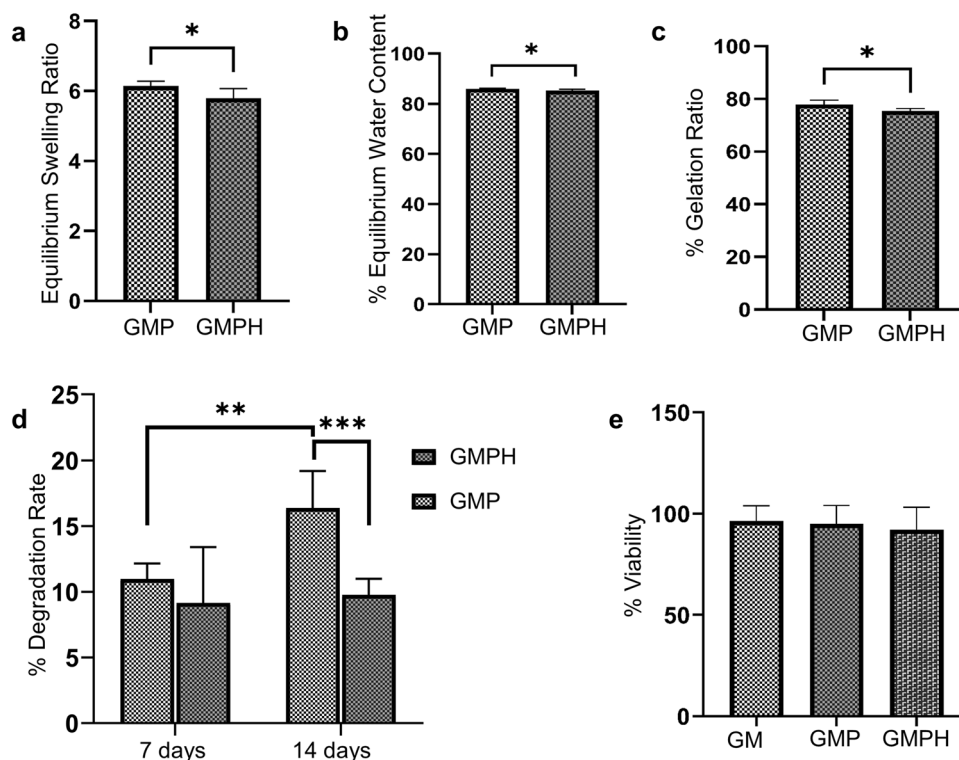


Fig. 4 Physical and biological properties of GMP/GMPH hydrogels. **a** Equilibrium swelling ratio (ESR) of GMP and GMPH hydrogels ($n=6$, unpaired two-tailed t test, $P=0.0195$, $*P<0.05$); **b** Equilibrium water content (EWC) of GMP and GMPH hydrogels ($n=6$, unpaired two-tailed t test, $P=0.0190$, $*P<0.05$); **c** Gelation ratio of GMP and GMPH hydrogels ($n=6$, unpaired two-tailed t test, $P=0.0114$, $*P<0.05$); **d** Biodegradation assay showed an acceler-

ated degradation rate (%) of GMP hydrogel in week 2 ($n=6$, unpaired two-tailed t test, $P=0.0015$, $*P<0.05$). GMPH hydrogel showed a slower degradation rate than GMP hydrogel in week 2 ($n=6$, unpaired two-tailed t test, $P=0.0004$, $*P<0.05$); **e** MTT assay showing the viability of MG63 cells treated with the extracts of hydrogels. All error bars represent mean \pm s.e.m. GM (GelMA), GMP (GelMA/PEGDA), GMPH (GelMA/PEGDA-nanohydroxyapatite)

In vitro degradation

Biodegradation plays a pivotal role in the biomaterial's long-term efficacy on tissue regeneration (Liao and Cui 2004). The hydrogel discs were treated with collagenase enzyme for two weeks to monitor the rate of degradation and stability. The degradation profile of GMP and GMPH hydrogels is summarized in Fig. 4d. It can be observed that the percentage decrease in dry weight of GMPH hydrogel was found to be comparatively lower than GMP hydrogel. Even though both the hydrogels showed a similar degradation profile in the first week, the percentage reduction in dry weight of GMPH hydrogels was lower than that of GMP in the second week, indicating a slower rate of degradation of GMPH hydrogel. Degradation of loosely bound GelMA polymers within the hydrogel network occurred during the first week of treatment, following which the hydrogels exhibited controlled degradation. The results demonstrated that GMP and GMPH hydrogels are stable in physiological conditions and that nanohydroxyapatite further preserves the stability of the hydrogel. The slower rate of GMPH scaffold degradation is highly beneficial in supporting new bone growth over a

long period (Barbeck et al. 2017). Thus, GMPH hydrogel can be considered suitable for scaffold-assisted bone tissue engineering.

Cytocompatibility

The degradative products and unreacted molecules in the polymeric composites can impart toxicity to cells limiting their use in vitro and in vivo applications. Proper cross-linking of the polymers leaving little or no unreacted components is essentially the most critical step in the hydrogel fabrication. Such a toxic response of the hydrogels can be evaluated by treating cells with hydrogel extracts. Metabolic assays or cell viability assays were carried out to confirm the cytocompatibility of the GMPH hydrogel. The percentage viability of MG63 cells treated with the hydrogel extracts was more than 95% compared to that of control, as shown in Fig. 4e. We have included 10% GelMA hydrogel in this assay for comparison and to assess the effect of increasing polymer concentration on viability. Overall, the data showed that hydrogels are not releasing any components that could harm the cells and that GMPH hydrogel is cytocompatible.

Conclusion

Nanohydroxyapatite reinforced GelMA/PEGDA (GMPH) hydrogel was synthesized by a facile blending and photocrosslinking approach. SEM analysis showed that GMPH hydrogel possesses a microporous internal architecture, an ideal environment for cell infiltration, and nutrients/gaseous transport. The studies on the hydrogels' swelling and gelation properties revealed that the incorporation of nanohydroxyapatite in the hydrogel as a nanofiller stabilizes GMPH hydrogel without disrupting network structure and properties. In vitro degradation results showed that the hydrogels are stable, and the incorporation of nanohydroxyapatite further stabilized the GMPH hydrogel by slowing down the degradation rate. Cell viability assay using MG63 osteoblasts showed that the GMPH hydrogel possessed excellent biocompatibility. Altogether, our study showed that GMPH hydrogel is suitable for engineering bone tissue and can be potentially used for cell-based and growth factor-based scaffold-assisted osteoregenerative therapy.

Acknowledgements The present study was supported by financial sources from the University of Kerala in the form of faculty research funds and PhD. fellowship. FTIR, NMR and SEM analyses were performed at the Central Laboratory for Instrumentation and Facilitation (CLIF), University of Kerala.

Compliance with ethical standards

Conflict of interest The authors declare that they have no conflict of interest to publish this manuscript.

Ethical approval This article does not contain any studies with human participants or animals performed by any authors.

References

- Abbasi N, Hamlet S, Love RM, Nguyen NT (2020) Porous scaffolds for bone regeneration. *J Sci* 5(1):1–9
- Barbeck ST, Booms P, Stojanovic S, Najman S, Engel E, Sader R, Kirkpatrick JC, Navarro M, Ghanaati S (2017) Analysis of the in vitro degradation and the in vivo tissue response to bi-layered 3D-printed scaffolds combining PLA and biphasic PLA/bioglass components—guidance of the inflammatory response as basis for osteochondral regeneration. *Bioactive Mater* 2(4):208–223. <https://doi.org/10.1016/j.bioactmat.2017.06.001>
- Bendtsen ST, Quinnell SP, Wei M (2017) Development of a novel alginate-polyvinyl alcohol-hydroxyapatite hydrogel for 3D bioprinting bone tissue engineered scaffolds. *J Biomed Mater Res* 105(5):1457–1468. <https://doi.org/10.1002/jbm.a.36036>
- Celikkin N, Mastrogiacomo S, Jaroszewicz J, Walboomers XF, Swieszkowski W (2018) Gelatin methacrylate scaffold for bone tissue engineering: the influence of polymer concentration. *J Biomed Mater Res* 106(1):201–209. <https://doi.org/10.1002/jbm.a.36226>
- Choi JR, Yong KW, Choi JY, Cowie AC (2019) Recent advances in photo-crosslinkable hydrogels for biomedical applications. *Biotechniques* 66(1):40–53. <https://doi.org/10.2144/btn-2018-0083>
- Fang X, Xie J, Zhong L, Li J, Rong D, Li X, Ouyang J (2016) Biomimetic gelatin methacrylamide hydrogel scaffolds for bone tissue engineering. *J Mater Chem B* 4(6):1070–1080. <https://doi.org/10.1039/c5tb02251g>
- Farokhi M, Mottaghtalab F, Shokrgozar MA, Ou KL, Mao C, Hosseinkhani H (2016) Importance of dual delivery systems for bone tissue engineering. *J Control Release* 225:152–169
- Gnanaprakasam Thankam F, Muthu J (2014) Alginate based hybrid copolymer hydrogels—influence of pore morphology on cell-material interaction. *Carbohydr Polym* 112:235–244. <https://doi.org/10.1016/j.carbpol.2014.05.083>
- Hamlet SM, Vaquette C, Shah A, Hutmacher DW, Ivanovski S (2017) 3-Dimensional functionalized polycaprolactone-hyaluronic acid hydrogel constructs for bone tissue engineering. *J Clin Periodontol* 44(4):428–437. <https://doi.org/10.1111/jcpe.12686>
- Hernández-González AC, Téllez-Jurado L, Rodríguez-Lorenzo LM (2020) Alginate hydrogels for bone tissue engineering, from injectables to bioprinting: a review. *Carbohydr Polym* 229:115514
- Hoch E, Schuh C, Hirth T, Tovar GEM, Borchers K (2012) Stiff gelatin hydrogels can be photo-chemically synthesized from low viscous gelatin solutions using molecularly functionalized gelatin with a high degree of methacrylation. *J Mater Sci* 23(11):2607–2617. <https://doi.org/10.1007/s10856-012-4731-2>
- Hoch E, Hirth T, Tovar GEM, Borchers K (2013) Chemical tailoring of gelatin to adjust its chemical and physical properties for functional bioprinting. *J Mater Chem B* 1(41):5675–5685. <https://doi.org/10.1039/c3tb20745e>
- Jabbarzadeh E, Blanchette J, Shazly T, Khademhosseini A, Camci-Unal G, Laurencin C (2012) Vascularization of biomaterials for bone tissue engineering: current approaches and major challenges. *Curr Angiogenesis* 1(3):180–191. <https://doi.org/10.2174/2211552811201030180>
- Jamróz E, Kulawik P, Kopel P (2019) The effect of nanofillers on the functional properties of biopolymer-based films: a review. *Polymers* 11(4):675
- Li J, Ebied M, Xu J, Zreiqat H (2018) Current approaches to bone tissue engineering: the interface between biology and engineering. *Adv Healthcare Mater* 7(6):1701061. <https://doi.org/10.1002/adhm.201701061>
- Liao SS, Cui FZ (2004) In vitro and in vivo degradation of mineralized collagen-based composite scaffold: Nanohydroxyapatite/Collagen/Poly(L-Lactide). *Tissue Eng* 10(1–2):73–80. <https://doi.org/10.1089/107632704322791718>
- Lin L, Chow KL, Leng Y (2009) Study of hydroxyapatite osteoinductivity with an osteogenic differentiation of mesenchymal stem cells. *J Biomed Mater Res* 89(2):326–335. <https://doi.org/10.1002/jbm.a.31994>
- Liu Y, Luo D, Wang T (2016) Hierarchical structures of bone and bioinspired bone tissue engineering. *Small* 12(34):4611–4632
- Liu M, Zeng X, Ma C, Yi H, Ali Z, Mou X, Li S, Deng Y, He N (2017) Injectable hydrogels for cartilage and bone tissue engineering. *Bone Res* 5:17014
- Lops D, Feroni L, Gardin CA, Ricci S, Guazzo R, Sbricoli L, Romeo E, Calvo-Guirado JL, Bressan E, Zavan BA (2014) Osteoproperties of polyethylene glycol hydrogel material. *J Osseointegr* 6(3):61–65. <https://doi.org/10.23805/jo.2014.06.03.04>
- Maisani M, Pezzoli D, Chassande O, Mantovani D (2017) Cellularizing hydrogel-based scaffolds to repair bone tissue: How to create a physiologically relevant micro-environment? *J Tissue Eng* 8:204173141712073. <https://doi.org/10.1177/204173141712073>
- Mohajeri S, Hosseinkhani H, Golshan Ebrahimi N, Nikfarjam L, Soleimani M, Kajibafzadeh A (2010) Proliferation and

- differentiation of mesenchymal stem cell on collagen sponge reinforced with polypropylene/polyethylene terephthalate blend fibers. *Tissue Eng Part A* 16(12):3821–3830. <https://doi.org/10.1089/ten.tea.2009.0520>
- Mottaghtalab F, Hosseinkhani H, Shokrgozar MA, Mao C, Yang M, Farokhi M (2015) Silk as a potential candidate for bone tissue engineering. *J Control Release* 215:112–128
- Nguyen TH, Ventura R, Min Y, Lee B (2016) Genipin cross-linked polyvinyl alcohol-gelatin hydrogel for bone regeneration. *J Biomed Sci Eng* 09(09):419–429. <https://doi.org/10.4236/jbise.2016.99037>
- Nurlidar F, Yamane K, Kobayashi M, Terada K, Ando T, Tanihara M (2018) Calcium deposition in photocrosslinked Poly(Pro-Hyp-Gly) hydrogels encapsulated rat bone marrow stromal cells. *J Tissue Eng Regen Med* 12(3):e1360–e1369. <https://doi.org/10.1002/term.2520>
- Pan Y (2010) Swelling properties of nano-hydroxyapatite reinforced Poly(Vinyl Alcohol) gel biocomposites. *Micro Nano Lett* 5(4):237–240. <https://doi.org/10.1049/mnl.2010.0061>
- Peppas NA, Hilt J, Khademhosseini A, Langer R (2006) Hydrogels in biology and medicine: from molecular principles to bionanotechnology. *Adv Mater* 18(11):1345–1360
- Peppas NA, Hoffman AS (2020) 1.3.2E - Hydrogels. In: Wagner WR, Sakiyama-Elbert SE, Zhang G, Yaszemski MJ (eds) *Biomaterials science*, 4th Edn. Academic Press, pp 153–166
- Perez JR, Kouroupis D, Li DJ, Best TM, Kaplan L, Correa D (2018) Tissue engineering and cell-based therapies for fractures and bone defects. *Front Bioeng Biotechnol*. <https://doi.org/10.3389/fbioe.2018.00105>
- Polo-Corrales L, Latorre-Esteves M, Ramirez-Vick JE (2014) Scaffold design for bone regeneration. *J Nanosci Nanotechnol* 14(1):15–56
- Radhakrishnan A, Jose GM, Kurup M (2015) PEG-penetrated chitosan-alginate co-polysaccharide-based partially and fully crosslinked hydrogels as ECM mimic for tissue engineering applications. *Progress Biomater* 4(2–4):101–112. <https://doi.org/10.1007/s40204-015-0041-3>
- Rahali K, Ben Messaoud Gh, Kahn CJF, Sanchez-Gonzalez L, Kaci M, Cleymand F, Fleutot S, Linder M, Desobry S, Arab-Tehrany E (2017) Synthesis and characterization of nanofunctionalized gelatin methacrylate hydrogels. *Int J Mol Sci*. <https://doi.org/10.3390/ijms18122675>
- Saberianpour S, Heidarzadeh M, Geranmayeh MH, Hosseinkhani H, Rahbarghazi R, Nouri M (2018) Tissue engineering strategies for the induction of angiogenesis using biomaterials. *J Biol Eng* 12(1):1–15
- Sadeghi M, Heidari B (2011) Crosslinked graft copolymer of methacrylic acid and gelatin as a novel hydrogel with PH-responsiveness properties. *Materials* 4(3):543–552. <https://doi.org/10.3390/ma4030543>
- Saldin LT, Cramer MC, Velankar SS, White LJ, Badylak SF (2017) Extracellular matrix hydrogels from decellularized tissues: structure and function. *Acta Biomater* 49:1–15
- Satpathy A, Pal A, Sengupta S, Das A, Hasan MM, Ratha I, Barui A, Bodhak S (2019) Bioactive nano-hydroxyapatite doped electrospun PVA-chitosan composite nanofibers for bone tissue engineering applications. *J Indian Inst Sci* 99(3):289–302
- Seliktar D (2012) Designing cell-compatible hydrogels for biomedical applications. *Science* 336(6085):1124–1128
- Shirahama H, Lee BH, Tan LP, Cho NJ (2016) Precise tuning of facile one-pot gelatin methacryloyl (GelMA) synthesis. *Sci Rep* 6(1):1–11. <https://doi.org/10.1038/srep31036>
- Stratton S, Shelke NB, Hoshino K, Rudraiah S, Kumbar SG (2016) Bioactive polymeric scaffolds for tissue engineering. *Bioactive Mater* 1(2):93–108
- Toosi Sh, Naderi-Meshkin H, Kalalinia F, HosseinKhani H, Heirani-Tabasi A, Havakhah S, Nekooei S, Jafarian AH, Rezaie F, Peivandi MT, Mesgarani H, Behravan J (2019) Bone defect healing is induced by collagen sponge/polyglycolic acid. *J Mat Sci* 30(3):1–10. <https://doi.org/10.1007/s10856-019-6235-9>
- Van Den Bulcke AI, Bogdanov B, De Rooze N, Schacht Eh, Cornelissen M, Berghmans H (2000) Structural and rheological properties of methacrylamide modified gelatin hydrogels. *Biomacromol* 1(1):31–38. <https://doi.org/10.1021/bm990017d>
- Wang Y, Ma M, Wang J, Zhang W, Lu W, Gao Y, Zhang B, Guo Y (2018) Development of a photo-crosslinking, biodegradable GelMA/PEGDA hydrogel for guided bone regeneration materials. *Materials*. <https://doi.org/10.3390/ma11081345>
- Wang Y, Cao X, Ma M, Lu W, Zhang B, Guo Y (2020) A GelMA-PEGDA-NHA composite hydrogel for bone tissue engineering. *Materials* 13(17):3735. <https://doi.org/10.3390/ma13173735>
- Yue K, Li X, Schrobback K, Sheikhi A, Annabi N, Leijten J, Zhang W, Zhang YS, Huttmacher DW, Klein TJ, Khademhosseini A (2017) Structural analysis of photocrosslinkable methacryloyl-modified protein derivatives. *Biomaterials* 139:163–171. <https://doi.org/10.1016/j.biomaterials.2017.04.050>

Publisher's Note Springer Nature remains neutral with regard to jurisdictional claims in published maps and institutional affiliations.

